Journal of Coastal Research	16	3	870–876	West Palm Beach, Florida	Summer 2000

Resonant Reflection of Waves over Sinusoidally Varying Topographies

Yong-Sik Cho† and Changhoon Lee‡

†Department of Civil Engineering
Hanyang University
Seoul 133-791, Korea

‡Department of Civil and Environmental Engineering
Sejong University
Seoul 143-747, Korea

ABSTRACT

CHO, Y. S. and LEE, C., 2000. Resonant reflection of waves over sinusoidally varying topographies. *Journal of Coastal Research,* 16(3), 870–876. West Palm Beach (Florida), ISSN 0749-0208.

The propagation of monochromatic waves over an arbitrarily varying topography is studied theoretically. The varying topography is first represented by a finite number of small steps. A theoretical model is then developed by formulating the diffraction of monochromatic waves by abrupt depth changes, through the eigenfunction expansion method. Not only the propagating mode but also the evanescent modes are included in the model. The model developed is applied to the study of the Bragg reflection of monochromatic waves caused by a singly-sinusoidally varying topography. The effects of the oblique incidence of waves are also investigated. The model solutions are compared with available experimental data. The model is also used to investigate the Bragg reflection of monochromatic waves over a doubly-sinusoidally varying topography. The reflection coefficients calculated are compared with laboratory measurements and other numerical results. A reasonable agreement is observed.

ADDITIONAL INDEX WORDS: *Water waves, eigenfunction expansion method, Bragg reflection, evanescent modes, sinusoidally varying topography.*

INTRODUCTION

As wind waves generated in deep water approach the nearshore zone, they experience many important physical phenomena caused by bathymetric variations, nonlinear interactions among different wave components and interferences with man-made coastal structures. Among these, the bathymetric variations play a significant role in the change of the wave climate. Thus, coastal engineers should have a proper tool for estimating the wave climate as accurately as possible to design a coastal structure in nearshore areas. In particular, the accurate calculation of reflection and transmission coefficients of incident waves over a local bottom topography is indispensible for proper and economical design of coastal structures.

The propagation of monochromatic surface waves over a submerged object or sand bars has been frequently and widely investigated through theoretical, experimental and numerical studies because of its practical applications in coastal morphology and designing of submerged breakwaters. Recently, an extensive literature review on linear wave scattering by two-dimensional bottom topography was given by PORTER and CHAMBERLAIN (1997).

Among theoretical studies, MILES (1967) used a scattering matrix method to calculate the reflection and transmission coefficients for the case of a step discontinuity between two finite depths. A scattering matrix obtained from the variation formulation was defined by relating the coefficients of the two propagating modes on each side of the step. KIRBY and DALRYMPLE (1983) calculated the reflection and transmission coefficients of monochromatic waves over a submerged trench by using an eigenfunction expansion method. The obtained solutions agree well with numerical solutions computed by the boundary integral equation method. DEVILLARD *et al.* (1988) used MILES' scattering matrix to calculate the reflection coefficients for the successive steps. Since the evanescent modes were not considered in the method, the lengths of the steps were large enough to ensure noncoupling between the evanescent modes created by the two successive steps.

Only a few experimental studies have been reported for the reflection of water waves over rippled beds. DAVIES and HEATHERSHAW (1984) conducted laboratory experiments on the propagation of monochromatic waves over a sinusoidally varying topography. They studied the so called Bragg resonant reflection. BENJAMIN *et al.* (1987) also reported a theoretical and experimental study for the Bragg reflection of long-crested surface waves over a sinusoidally varying topography to reveal the development of coastal sandbars. They argued that the study may improve DAVIES and HEATHERSHAW's investigation in a few respects. Recently, GUAZZELLI *et al.* (1992) studied the higher-order Bragg reflection caused by doubly-sinusoidally varying topography. REY *et al.* (1992) performed a series of laboratory experiments for the propagation of linear and weakly nonlinear waves over a rectangular submerged bar. The measured data were compared with both KIRBY and DALRYMPLE's and DEVILLARD *et al.*'s theoretical solutions. They demonstrated the importance of the evanescent modes by examining the experimental behav-

98277 received 30 December 1998; accepted in revision 27 September 1999.

ior of the fundamental wave amplitude over the submerged bed.

Numerical models were also plausibly used to calculate the reflection and transmission coefficients over a special bottom topography. LIU and ABBAPOUR (1982) studied the diffraction of obliquely incident waves by an infinite number of cylinders with the boundary integral equation method. DALRYMPLE and KIRBY (1986) also used the boundary integral equation method to study the interaction between small amplitude waves and a series of seabed ripples. The numerical solutions obtained were compared with the laboratory measured data of DAVIES and HEATHERSHAW (1984).

Recently, O'HARE and DAVIES (1992) presented a new method for the modeling of propagation of monochromatic waves over a smoothly varying bottom topography. A similar technique was also used by GUAZZELLI *et al.* (1992). They first divided the topography into a series of small steps and calculated the reflection coefficient by using MILES' scattering matrix method. They proved the accuracy and validity of the method by comparing the reflection and transmission coefficients obtained for both single and double steps with theoretical solutions calculated by the eigenfunction expansion method. However, the method is applied only to normally incident waves to the bottom topography. Furthermore, the effects of evanescent modes are not considered in the study.

In this study, we will develop a theoretical model based on the eigenfunction expansion method used by KIRBY and DALRYMPLE (1983) and LIU *et al.* (1992) to simulate the propagation of monochromatic waves over an arbitrary bathymetry. Following O'HARE and DAVIES (1992) and GUAZZELLI *et al.* (1992), we first divide the topography into a finite number of small steps. However, the evanescent modes as well as the propagating modes are considered in this study. Moreover, the effects of both normal and oblique incidence of surface waves are examined. Thus, O'HARE and DAVIES' and GUAZZELLI *et al.*'s studies can be viewed as a limited case of the present study.

In the following section, we first summarize the diffraction of monochromatic waves over an arbitrarily varying bottom topography. The theoretical model developed is then tested with several examples with different bottom topographies. Finally, concluding remarks are presented.

DIFFRACTION OF MONOCHROMATIC WAVES

In this section, the diffraction of monochromatic waves by a depth discontinuity is first given briefly for completeness. As shown in Figure 1, the bottom topography is first divided into a finite number of small steps. Variation of the bottom topography is limited to the x-direction and thus, the wave number in the y-direction remains constant throughout the study. Following KIRBY and DALRYMPLE (1983), the velocity potential functions of small amplitude waves within each region can be written as

$$\Phi_m^r = \left[A_m^r e^{+il_m x}\cosh k_m(h_m + z) + \sum_{n=1}^{\infty} B_{m,n}^r e^{+\lambda_{m,n}x}\cos K_{m,n}(h_m + z)\right]e^{i(k_y y-\omega t)} \quad (1)$$

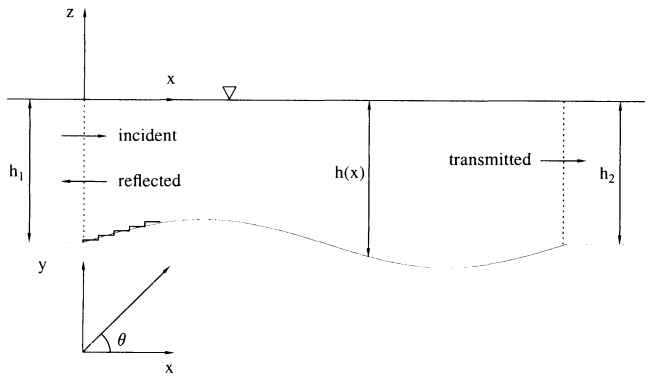

Figure 1. A schematic sketch of an arbitrarily varying topography.

for the right-going wave components and evanescent modes and

$$\Phi_m^l = \left[A_m^l e^{-il_m x}\cosh k_m(h_m + z) + \sum_{n=1}^{\infty} B_{m,n}^l e^{-\lambda_{m,n}x}\cos K_{m,n}(h_m + z)\right]e^{i(k_y y-\omega t)} \quad (2)$$

for the left-going wave components and evanescent modes. In equations (1) and (2), A_m^r, $B_{m,n}^r$, A_m^l and $B_{m,n}^l$ are complex amplitude functions to be determined and the subscripts m and n represent the number of regions and the number of evanescent modes to be considered, respectively. Also, z is the vertical coordinate (see Figure 1), h_m is the water depth in mth region and ω is the angular frequency. The superscripts r and l denote right- and left-going waves, respectively.

In equations (1) and (2), l_m and $\lambda_{m,n}$ are the wavenumber components in the x-direction for the propagating and evanescent modes, respectively. They are calculated from the relations given as:

$$k_m^2 = l_m^2 + k_y^2, \quad \lambda_{m,n}^2 = K_{m,n}^2 + k_y^2 \quad (3)$$

in which k_y is the wavenumber component in the y-direction. As mentioned previously, k_y remains constant over the whole domain because the variation in the topography is limited only to the x-direction. The wavenumbers at the mth region represented by k_m and $K_{m,n}$ are calculated from the dispersion relations given as:

$$\omega^2 = gk_m\tanh k_m h_m, \quad \omega^2 = -gK_{m,n}\tan K_{m,n}h_m \quad (4)$$

To solve equations (1) and (2) at each region, two matching conditions are required at each depth discontinuity. The first condition is expressed as:

$$\frac{\partial\Phi_i}{\partial x} = \frac{\partial\Phi_{i+1}}{\partial x}, \quad x = x_i, \quad \max(-h_i, -h_{i+1}) \le z \le 0 \quad (5)$$

which ensures the continuity of horizontal flux in the x-direction. The second condition is given as:

$$\Phi_i = \Phi_{i+1}, \quad x = x_i, \quad \max(-h_i, -h_{i+1}) \le z \le 0 \quad (6)$$

which guarantees the continuity of pressure.

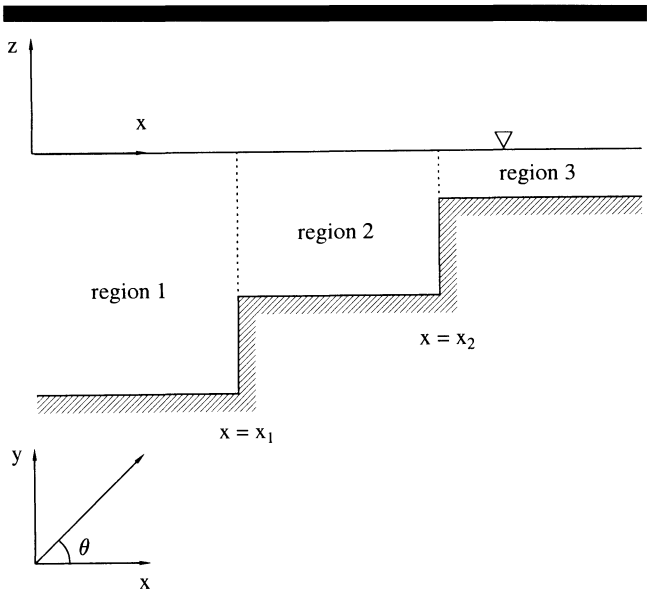

Figure 2. A schematic sketch of a backward double step.

Equations (5) and (6) can be solved by the eigenfunction expansion method. A detailed description of the method can be found in more detail in KIRBY and DALRYMPLE (1983).

NUMERICAL EXAMPLES

In this section, we investigate the reflection coefficients of monochromatic waves over steps and sinusoidally varying topographies. The occurrence of the Bragg reflection is studied in detail. Variations of reflection coefficients are also examined for different incident angles. Although the evanescent modes may not play a significant role in the determination of the reflection coefficients, if the size of each small step is properly controlled (O'HARE and DAVIES, 1992), they are included in this study. The reflection and transmission coefficients are defined as

$$R = |A_1^l|, \qquad T = \frac{\cosh k_m h_m}{\cosh k_1 h_1} |A_m^r| \tag{7}$$

Double Steps

We first apply the developed model to forward and backward double steps (see Figure 2) to verify accurate performance of the model. By definition the depth increases as x increases in the forward double step ($h_1 < h_2 < h_3$), while it decreases in the backward double step ($h_1 > h_2 > h_3$) as shown in Figure 2. For simplicity, the water depths are fixed as $h_2 = 2h_1$ and $h_3 = 3h_1$ in the forward step, while they are fixed as $h_2 = h_1/2$ and $h_3 = h_1/3$ in the backward step. The width of the step is fixed as $w = 2h_3$ in the forward step and $w = 2h_1$ in the backward step.

The reflection (R) and transmission (T) coefficients are calculated and listed in Table 1. In Table 1, n represents the number of evanescent modes considered in the model. Thus, $n = 0$ refers to the plane wave approximation. The variation of the reflection coefficients between $n = 0$ and $n = 2$ clearly shows the role of the evanescent modes. That is, the transmission coefficients decrease slightly as n increases, whereas reflection coefficients increase slightly. For all the cases, the wave energy is found to be conserved. It should be noted that the matrix becomes large and the computational efficiency may decrease for a succession of steps. However, all the computations reported in this paper were still endurable in a workstation.

A Singly-Sinusoidally Varying Topography

In this example the model is used to calculate the resonant and nonresonant reflection coefficients over a sinusoidally varying topography. The bottom topography is also represented by a series of small steps. The water depth is defined as

$$\begin{aligned} h(x) &= h_1, && x < x_1 \\ h(x) &= h_1 - b \sin(lx), && x_1 \le x \le x_2 \\ h(x) &= h_1, && x > x_2 \end{aligned} \tag{8}$$

in which b and l are the amplitude and the wavenumber of the seabed ripple, respectively. A wavelength of the sinusoidal ripple is represented by 200 small steps as also done by O'HARE and DAVIES (1992). Two cases, one ($n = 0$) with the propagating mode only and the other ($n = 4$) with the four evanescent modes as well as the propagating mode, are considered in the calculation. Numerical solutions of the reflection coefficient are compared with the experimental data of DAVIES and HEATHERSHAW (1984).

Two cases, one ($m = 2$) with two ripples and the other ($m = 4$) with four ripples are tested and comparisons are made in Figures 3 and 4, respectively. For both cases, the amplitude of the seabed ripple is $b = 0.32h_1$. Another case ($m = 10$) with ten ripples are tested and comparisons are made in Figure 5. For this case, $b = 0.16h_1$. In the figures k is the wavenumber of the incident wave. Inclusion of the evanescent modes causes reflections to occur at lower wavenumbers. It is noticeable that wave reflections at the second-order resonance ($2k/l \approx 2$) are reduced to almost zero when the evanescent modes are included in the calculations. As confirmed by CHO *et al.* (1997) the reflection coefficient becomes larger as the number of ripples increases. Away from the peak, the

Table 1. *Comparison of transmission and reflection coefficients for double steps* ($k_1h_1 = 0.75$, $\theta = 0°$).

Description	$n = 0$	$n = 2$	$n = 4$	$n = 8$	$n = 16$
forward—T	1.18775273	1.18261064	1.18229425	1.18207029	1.18200805
forward—R	0.20333157	0.22276964	0.22390794	0.22471002	0.22493236
backward—T	0.96031712	0.95649490	0.95614382	0.95598822	0.95592902
backward—R	0.07078085	0.11364253	0.11678659	0.11815288	0.11866856

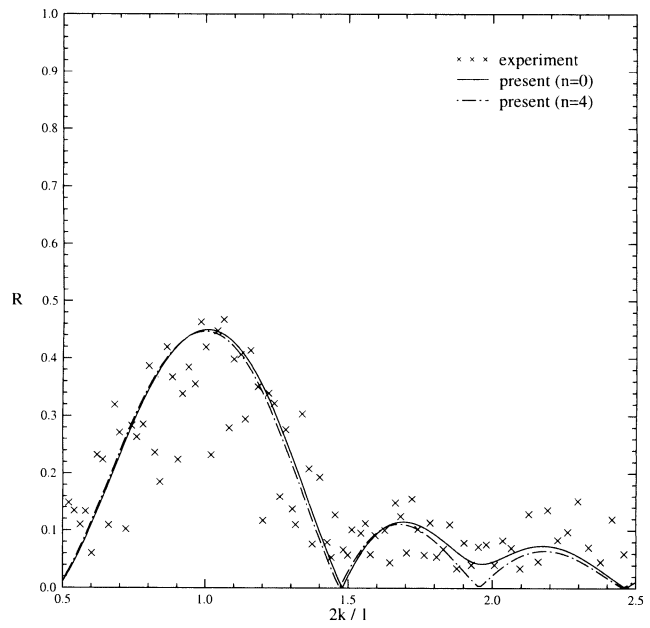

Figure 3. Variations of the reflection coefficients over a singly-sinusoidally varying topography ($m = 2$, $\theta = 0°$, $b/h_1 = 0.32$).

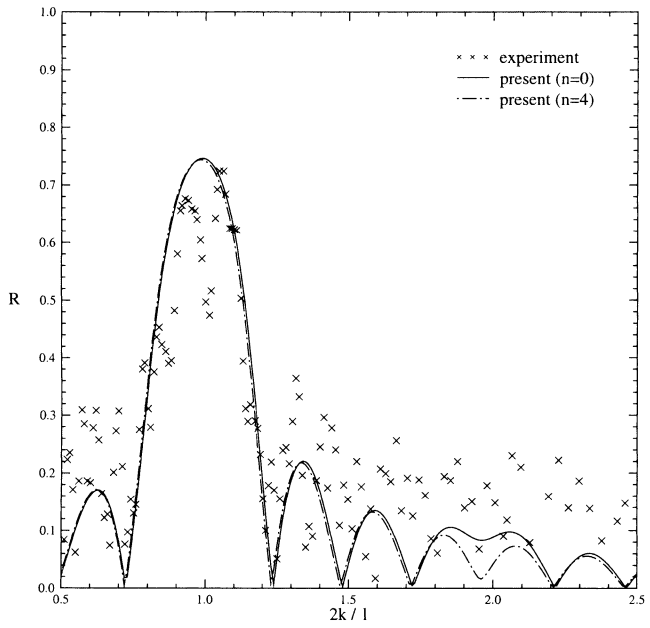

Figure 4. Variations of the reflection coefficients over a singly-sinusoidally varying topography ($m = 4$, $\theta = 0°$, $b/h_1 = 0.32$).

calculated coefficients are roughly half of the measured values. This discrepancy may be due to experimental errors. The overall agreement between the laboratory measurements and the computed solutions is reasonable.

The model is also used to calculate the reflection coefficients for obliquely incident waves which were not considered in O'HARE and DAVIES (1992) and GUAZZELLI *et al.* (1992). Figure 6 displays variations of the reflection coefficients for different incident angles with the same parameters used in Figures 3 and 4. For the case of $\theta = 30°$, the peaks are shifted to higher wavenumbers and the magnitude of reflections becomes smaller compared to the case of $\theta = 0°$. According to DALRYMPLE and KIRBY (1986) the wavenumber ratio for the obliquely incident wave is given as $2k \cos \theta/l = 1$ for the Bragg reflection. In Figure 6, the maximum reflections occur at $2k/l = 1$ for $\theta = 0°$, while they occur at $2k/l \approx 1.15$ for $\theta = 30°$. This agrees well with Dalrymple and Kirby's theoretical predictions. Thus, the present model can be applied to obliquely as well as normally incident waves. As the angle θ increases, the peaks are shifted to higher wavenumbers. This is because the wavelengths of incident waves become longer as the angle θ increases.

A Doubly-Sinusoidally Varying Topography

Finally, the developed model is employed to simulate the diffraction of monochromatic waves over a doubly-sinusoidally varying topography. The bottom topography is described as

$$\begin{aligned} h(x) &= h_1, && x < x_1 \\ h(x) &= h_1 - b[\sin(l_1 x) + \sin(l_2 x)], && x_1 \le x \le x_2 \\ h(x) &= h_1, && x > x_2 \end{aligned} \tag{9}$$

in which h_1 is a constant water depth, b is the ripple amplitude taken the same for both ripples of different wavelengths (λ_1 and λ_2), l_1 and l_2 are the wavenumbers of the longer and shorter ripples, respectively, and $x_2 - x_1 = L$ is the length of the rippled seabed. In the case of a rippled seabed consisting

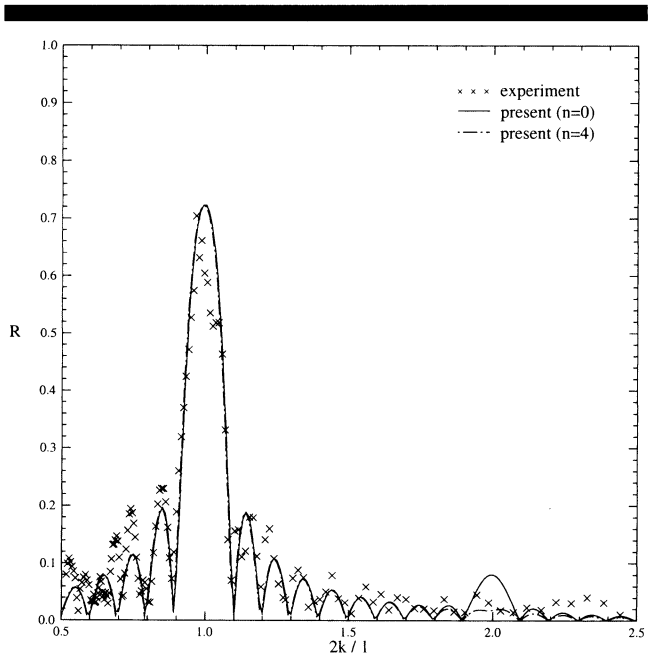

Figure 5. Variations of the reflection coefficients over a singly-sinusoidally varying topography ($m = 10$, $\theta = 0°$, $b/h_1 = 0.16$).

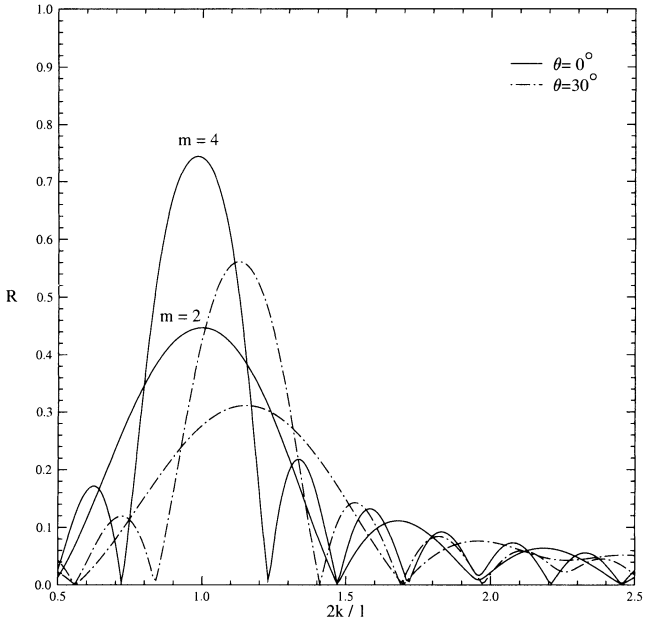

Figure 6. Variations of the reflection coefficients over a singly-sinusoidally varying topography ($n = 4$, $b/h_1 = 0.32$).

of the superposition of two sinusoidally-varying topographies having different wavenumbers with $l_2 > l_1$, GUAZZELLI *et al.* (1992) demonstrated that first-order Bragg reflections occur in the vicinities of $2k = l_1$ and $2k = l_2$, while second-order Bragg reflections occur near $2k = 2l_1$, $2k = 2l_2$ and $2k = l_1 + l_2$ for harmonic Bragg reflections and $2k = l_1 - l_2$ for sub-harmonic Bragg reflections. They also showed that the resonant peaks are slightly shifted towards a wavenumber lower than the predicted values.

Table 2. *Dimensions of doubly-sinusoidally varying topographies.*

Description	$h_1 = h_2$ (cm)	b (cm)	λ (cm)	λ_2 (cm)	L (cm)
Figure 7 (a)	2.5	1.0	12.0	6.0	48.0
Figure 7 (b)	4.0	1.0	12.0	6.0	48.0
Figure 8 (a)	2.5	1.0	6.0	4.0	48.0
Figure 8 (b)	4.0	1.0	6.0	4.0	48.0

In Figures 7 and 8, the calculated reflection coefficients are compared against other numerical results computed from the extended mild-slope equation (SUH *et al.*, 1997). The experimental data (GUAZZELLI *et al.*, 1992) are also plotted for comparison. Dimensions of the bottom topographies are listed in Table 2. Reflections are strengthened by the relative amplitude (b/h_1) of the seabed ripple. That is, the reflection coefficients in Figures 7 (a) and 8 (a) are much larger that those of Figures 7 (b) and 8 (b), because the relative amplitude of the ripple becomes larger. The reflection coefficients obtained by the extended mild-slope equations do not decrease even at a higher-wavenumber of $2k/l_1$, especially in Figure 8 (a). The reason is not clear at this stage. Inclusion of the evanescent modes yields solutions closer to the measured data especially in both harmonic and sub-harmonic resonances. The overall agreement between the present solutions and the results computed from the extended mild-slope equation is good.

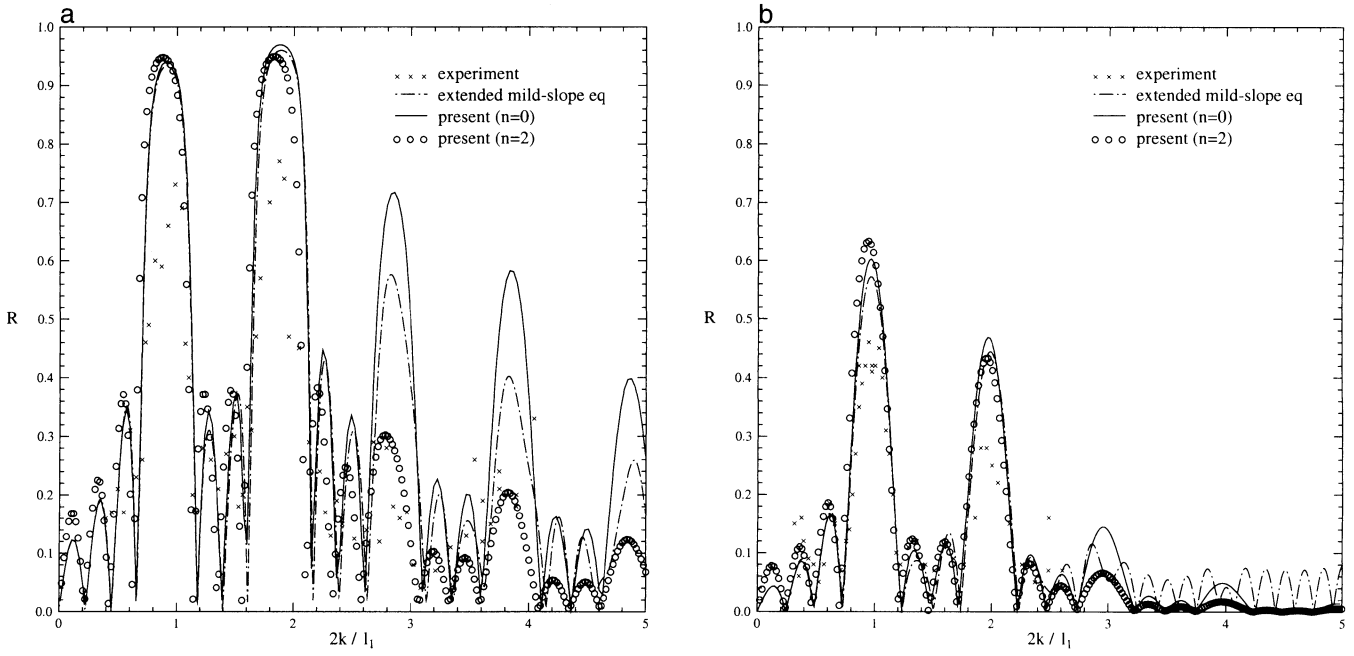

Figure 7(a). Reflection coefficients over a doubly-sinusoidally varying topography ($h_1 = h_2 = 2.5$cm, $b = 1.0$cm, $\lambda_1 = 12.0$cm, $\lambda_2 = 6.0$cm, $L = 48.0$cm).

Figure 7(b). Reflection coefficients over a doubly-sinusoidally varying topography ($h_1 = h_2 = 4.0$cm, $b = 1.0$cm, $\lambda_1 = 12.0$cm, $\lambda_2 = 6.0$cm, $L = 48.0$cm).

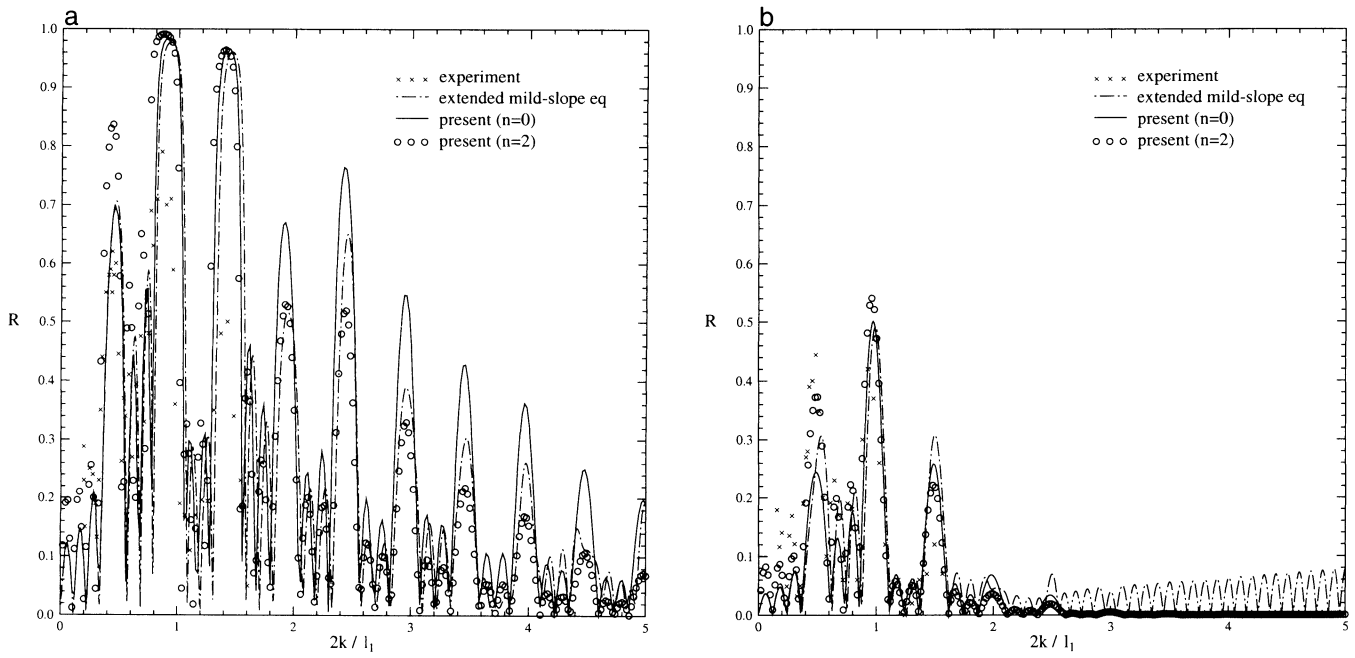

Figure 8(a). Reflection coefficients over a doubly-sinusoidally varying topography ($h_1 = h_2 = 2.5$cm, $b = 1.0$cm, $\lambda_1 = 6.0$cm, $\lambda_2 = 4.0$cm, $L = 48.0$cm).

Figure 8(b). Reflection coefficients over a doubly-sinusoidally varying topography ($h_1 = h_2 = 4.0$cm, $b = 1.0$cm, $\lambda_1 = 6.0$cm, $\lambda_2 = 4.0$cm, $L = 48.0$cm).

CONCLUDING REMARKS

A theoretical model describing the diffraction of monochromatic waves by abrupt depth changes is developed through the eigenfunction expansion method. The developed model is applied to the study of the Bragg reflection over sinusoidally varying topographies. The effects of the evanescent modes as well as the propagating mode are included in the model. Furthermore, the incident angle of monochromatic waves is not limited to the normal. The reflection coefficients calculated are compared with laboratory experimental data and numerical solutions of the existing model. Reasonable agreement is observed.

Although the representation of the bottom topography by a finite number of small steps requires a little more computational efforts and computing time, it is worth it to calculate the reflection coefficients over an arbitrarily varying topography as accurately as possible because of its important applications in designing coastal structures and preventing unwanted beach erosion and deposition.

The developed model can be used as a powerful tool for design in submerged breakwaters which can protect coastal structures and unwanted beach erosion by reflecting a significant amount of incident wave energy.

ACKNOWLEDGMENTS

The experimental data for singly- and doubly-sinusoidally varying topographies were gratefully provided by Professors T. J. O'Hare of the University of Plymouth and K. D. Suh of Seoul National University, respectively. This research was supported, in part, by research grants from the Korea Science and Engineering Foundation (981-1204-012-2).

LITERATURE CITED

BENJAMIN, T.B.; BOCAZAR-KARAKIEWICZ, B., and PRITCHARD, W.G., 1987. Reflection of water waves in a channel with corrugated bed. *Journal of Fluid Mechanics,* 185, 249–274.

CHO, Y.-S.; LEE, J.-I., and LEE, J.-K., 1997. Bragg reflection of shallow-water waves on a sloping beach. *Proceedings of the 25th International Conference on Coastal Engineering (ASCE)*, pp. 955–967.

DAVIES, A.G. and HEATHERSHAW, A.D., 1984. Surface-wave propagation over sinusoidally varying topography. *Journal of Fluid Mechanics,* 144, 419–443.

DALRYMPLE, R.A. and KIRBY, J.T., 1986. Water waves over ripples. *Journal of Waterway, Port, Coastal, and Ocean Engineering,* ASCE, 112, 309–319.

DEVILLARD, P.; DUNLOP, F., and SOUILLARD, B., 1988. Localisation of gravity waves on a channel with a random bottom. *Journal of Fluid Mechanics,* 186, 521–538.

GUAZZELLI, E.; REY V., and BELZONS, M., 1992. Higher-order Bragg reflection of gravity surface waves by periodic beds. *Journal of Fluid Mechanics,* 245, 301–317.

KIRBY, J.T. and DALRYMPLE, R.A., 1983. Propagation of obliquely incident water waves over a trench. *Journal of Fluid Mechanics,* 133, 47–63.

LIU, P.L.-F. and ABBASPOUR, M., 1982. An integral equation method for the diffraction of oblique waves by an infinite cylinder. *International Journal of Numerical Methods in Engineering,* 18, 1497–1504.

LIU, P.L.-F.; CHO, Y.-S.; KOSTENSE, J.K., and DINGEMANS, M.W. 1982. Propagation and trapping of obliquely incident wave groups over a trench with currents. *Applied Ocean Research,* 14, 201–212.

MILES, J.W., 1967. Surface wave scattering matrix for a shelf. *Journal of Fluid Mechanics,* 28, 755–767.

O'HARE, T.J. and DAVIES, A.G., 1992. A new model for surface-wave propagation over undulating topography. *Coastal Engineering,* 18, 251–266.

PORTER, D. and CHAMBERLAIN, P.G., 1997. Linear wave scattering by two-dimensional topography, *In:* HUNT, J.N. (ed.), *Gravity Waves of Finite Depth.* Computational Mechanics Publications, pp. 13–53.

REY, V.; BELZONS, M., and GUAZZELLI, E., 1992. Propagation of surface gravity waves over a rectangular submerged bar. *Journal of Fluid Mechanics,* 235, 453–479.

SUH, K.D.; LEE, C., and PARK W.S., 1997. Time-dependent equations for wave propagation on rapidly varying topography. *Coastal Engineering,* 32, 91–117.